Russ. J. Earth. Sci., Vol. 22, ES2003
https://doi.org/10.2205/2022ES000793

Freezing of Tidal Current Under Ice in a Shallow Channel

E. G. Morozov*[1,2], A. V. Marchenko[3], and K.V. Filchuk[4]

[1] *Shirshov Institute of Oceanology, Russian Academy of Sciences, Moscow, Russia*
[2] *Marine Hydrophysical Institute of RAS, Sevastopol, Russia*
[3] *The University Center in Svalbard, Longyearbyen, Spitsbergen, Norway*
[4] *Arctic and Antarctic Research Institute, St. Petersburg, Russia*

Received 24 February 2022; accepted 21 March 2022; published 4 May 2022.

We analyze tidal currents under ice in a shallow channel located near the tip of the Van Mijen Fjord in Spitsbergen. During the flood cycle of tide seawater flows under ice and strongly freezes in a shallow channel. During the ebb cycle salinity of the outflowing water is greater than that of the inflowing water. Salt balance is estimated. During high-water tide, salt water seeps through the cracks in the ice to the surface, which increases salinity of the snow and water mixture.

Keywords: Spitsbergen, shallow water, channel under ice, tidal current, freezing of seawater, salinity increase

Citation: E. G. Morozov, A. V. Marchenko, and K.V. Filchuk, (2022), Freezing of tidal current under ice in a shallow channel, *Russ. J. Earth. Sci.*, Vol. 22, ES2003, 10.2205/2022ES000793.

Introduction

We study tidal currents under ice in a shallow tip of the Van Mijen Fjord in Spitsbergen. The location is called Braganzavägen. A creek of freshwater is flowing down from melting mountain snow and glaciers along the Kjellstromdalen valley to the southwest approximately along the middle line of the valley. This geological structure continues in a shallow channel (~1 m depth) in the Braganzavägen basin. This basin is subjected to strong tides in the Van Mijen Fjord. The open ocean is located at a distance of 80 km. The basin is covered with ice in winter. The whole bulk of ice in the basin is generally aground because most of the basin area freezes to the bottom. However, continuations of the flow from the mountains along shallow channels do not freeze to the bottom in February leaving a shallow channel that allows a tidal flow.

A summer aerial photo in Figure 1 shows the stream from the mountains in the valley, which flows into the fjord in the shallow Braganzavägen basin. Another aerial photo of this region is also shown in Figure 1. A chart of the region is shown in Figure 2.

Tidal currents flow into these channels, which leads to the periodical elevations and depressions of the ice cover along these channels. Tidal currents generally follow the middle channel in the basin. Previous researches in this region are reported in [*Bogorodskii et al.*, 2020; *Marchenko et al.*, 2010, 2013, 2021; *Marchenko and Morozov*, 2016; *Morozov et al.*, 2019, 2011] The works on ice in the Van Mijen Fjord were reported in [*Skarðhamar and Svendsen*, 2010; *Høyland*, 2009]. Ice regime and tides were studied by *Høyland and Løset* [1999], *Liferov et al.* [2004] *Høyland and Liferov* [2005] and *Strub-Klein and Høyland* [2012] *Moslet* [2008] performed medium scale ice-structure interaction experiment in the Van Mijen Fjord. Ice thermodynamics was studied in [*Launiainen et al.*, 1998; *Leppäranta*, 1993]. The work by *Cottier et al.* [2010] is a good review of processes in many fjords.

Data and Methods

Our measurements were conducted in the beginning of March, 2016. We found locations of these channels by drilling holes in the ice. Generally, the drill hit land after drilling the ice. During the ebb tide we saw depressions in the ice cover. After drilling ice at these locations, we found water under ice. During high water periods (flood) of tides these depressions disappeared and water under ice became deeper. One of these locations is marked with a red dot in Figure 2. Its coordinates are 77°54.322'N, 16°50.922'E. The thickness of the water layer under ice in this channel ranges from 50 to 70 cm. The width of the channel is approximately 35–40 m. The channel is 1.2 m deep relatively to the upper boundary of the ice cover (water level).

*Corresponding author: egmorozov@mail.ru

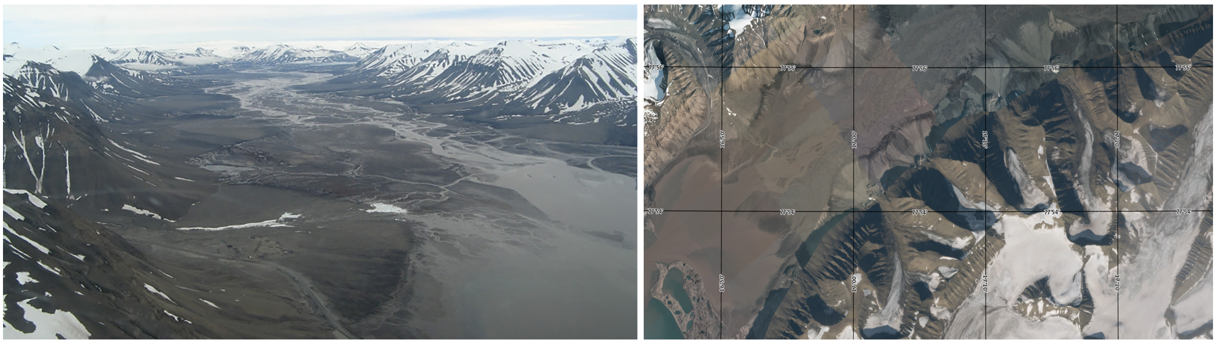

Figure 1: Photos of the region.

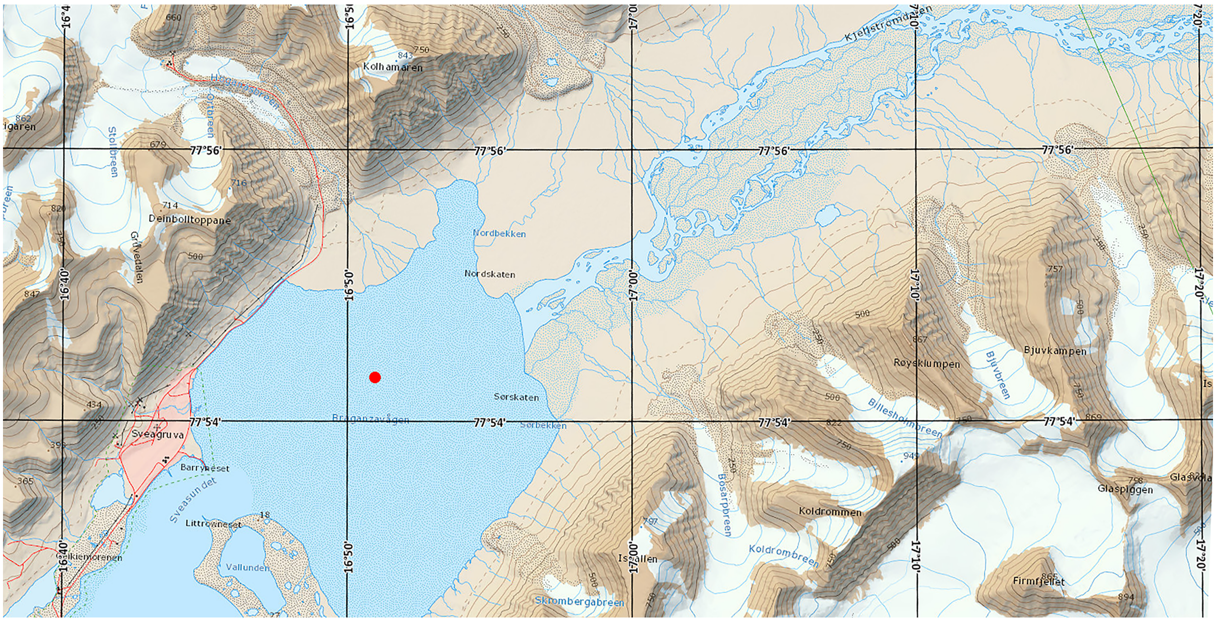

Figure 2: Chart of the region. The red dot indicates location of measurements.

We made a section of 10 holes across this channel to reveal the horizontal structure of the channel. This section was repeated several times during the high and low water tide. Then, we deployed an SBE-37 instrument in the deepest place on the bottom. The instrument measured pressure, temperature, and salinity. Ice thickness was measured with a graduated rod. A few temperature and salinity meters (Star-Oddi) were frozen in the ice at the surface. During high tide, water seeped to the surface and we could record salinity time series.

Discussion

Possible locations of the channels in Braganzavägen were reported in [*Shestov et al.*, 2015] based on field works Figure 3.

In March 2016, we made a section in the BV-1 region. A section of the channel bottom and ice cover during high and low water are shown in Figure 4.

One can see from Figure 4 that depression of ice cover during low water is well pronounced. The depth of the ice depression is almost 20 cm. Hence, it is clearly visible on the ice surface. Records of pressure and salinity measured by SBE-37 instrument at the bottom are shown in Figure 5 together with the records of surface salinity by the Star-Oddi sensors.

It is clearly seen from the records that during the flood period of the tide (increasing pressure) salinity of the inflowing water decreases because water is transported from the open regions of the fjord. During the ebb period of the tide (decreasing pressure) water flows from the channel to the fjord. Part of the water was frozen under ice and brine was released into water, thus increasing salinity of the outflowing stream.

During the high-water period, water seeped to the surface that caused increased salinity at the ice surface. Star-Oddi sensor recorded salinities within 10–12 psu. Let us estimate the increment of ice thickness during a tidal period, which is caused by partial freezing of seawater flowing into the channel. After freezing, salinity of the outflowing becomes greater.

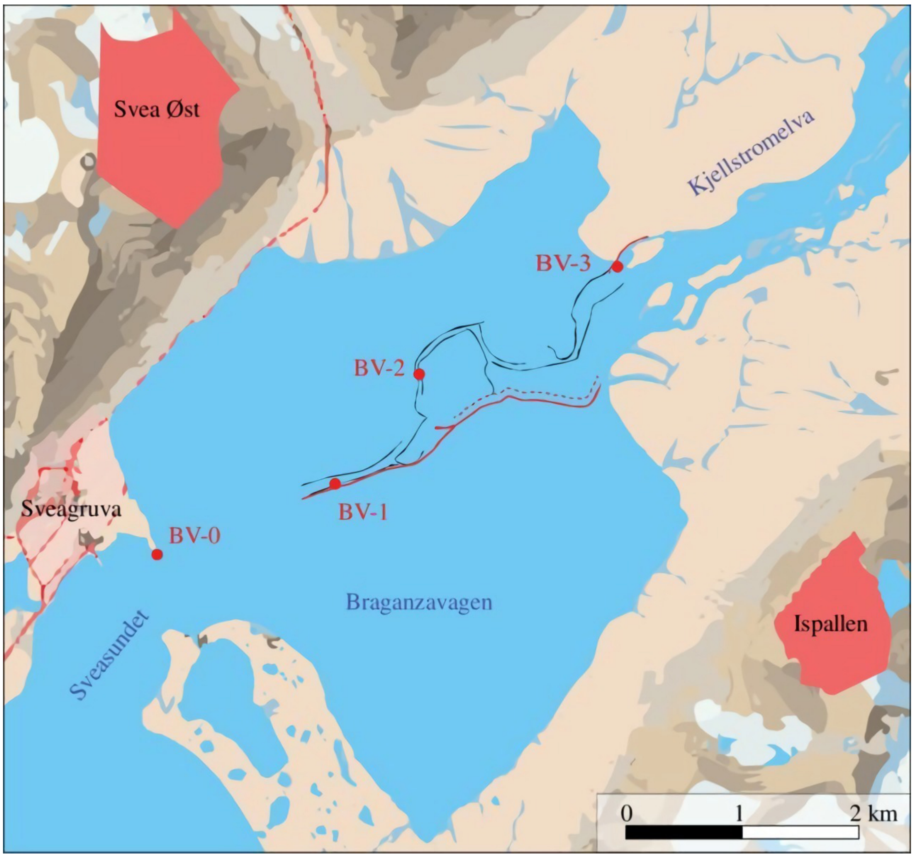

Figure 3: Locations of studies in 2014–2015. GPS recorded tracks (solid lines) of observed cracks in the ice in the Braganzavägen basin are shown. BV0, BV1, BV2, and BV3 are points of CTD measurements in 2014–2015 [*Shestov et al.*, 2015].

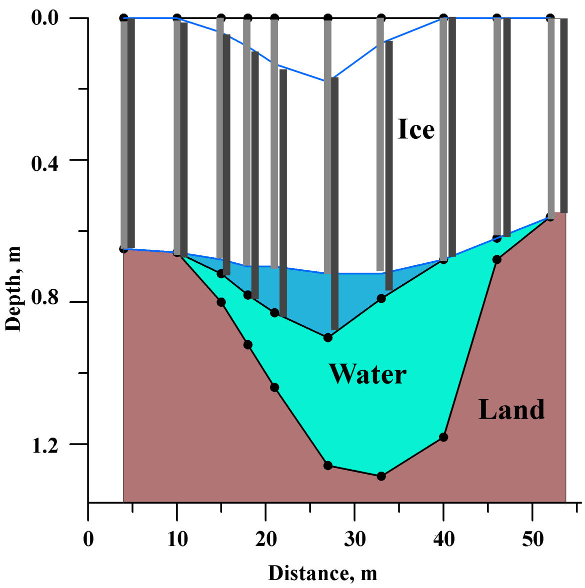

Figure 4: Section across the channel. Gray vertical lines show drillings through ice during high water and those of black color are related to low water. Ice is shown in two positions: high water (flat) and low water (depression). Land is shown with brown color.

Stefan [1891] recommended the following formula for practical calculations of ice thickness in time:

$$\sqrt{2 \cdot 86{,}400 \cdot \ \lambda \cdot \ \Sigma T j/(L \cdot \rho)},$$

where, 86,400 is the number of seconds during 24 hours, λ= 2.2 W (m°C) is coefficient of thermal conductivity of ice; ρ = 920 kg/m^3 is ice density; ΣT_j is the sum of degrees of frost multiplied by the number of days; $L = 3.3 \times 10^5$ J/kg is heat of fusion of ice. If we approximately assume that the ice thickness has been formed during 50 days at a temperature of −10°C, we get 79 cm, which is reasonable. The daily increment at a temperature of −10°C is 1 cm. This channel continues to the northeast from the location of the section. We also placed an SBE-37 instrument there at a distance of approximately 1000 m from the section. The water layer under ice was quite thin, approximately 10–15 cm. After 12 days we tried to recover it, but it was already covered with aground ice. The instrument was damaged during recovery.

Thus, we can calculate the amount of water transported by the tidal flow across our section during 6 hours. The cross-section of the water during high-water tide is 10 m^2. It decreases by 3 m^2 at the low-water tide. The square of the

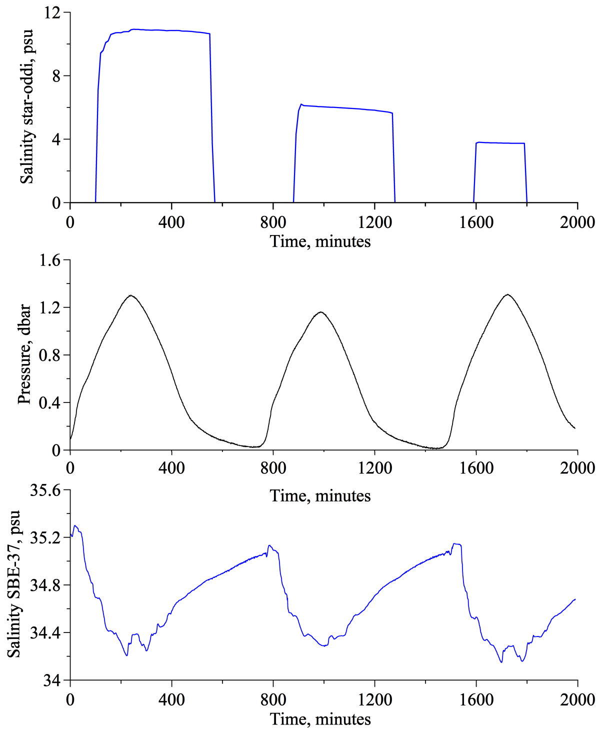

Figure 5: Time series of salinity at the surface measured by a Star-Oddi sensor (top panel); pressure at the bottom (middle panel) and salinity (bottom panel) measured by SBE-37.

channel surface (upper boundary of water) is approximately (40 m ·1000 m)/2 = 20,000 m^2. Water thickness difference between high and low water is 0.15 m. We assume that the channel becomes narrower in the northeastern direction (divide by 2). Thus, the amount of water transported to the northwest across the section during 6 hours is 3000 m^3. Knowing that the square of the cross-section is 10 m^2, the velocity of the current is estimated at 3000 m^3/(21,600 s ·10 m^2) = 0.014 m/s, which is a reasonable velocity.

The ice becomes thicker by 0.005 m during 12 hours of the tidal cycle, which makes 20,000 m^2 · 0.005 m = 100 m^3 of new ice.

Thus, 3000 m^3 of water with salinity 34.5 is transported to the northeast during the flood tide (6 hours). The amount of transported salt is 3000 m^3 · 34.2 kg/m^3 = 102,600 kg.

We assume that ice salinity is 5. The amount of salt frozen in the ice (5 kg/m^3) is 100 m^3·5 kg/m^3 = 500 kg. The volume of outflowing water is 100 m^3 smaller and amounts to 2900 m^3.

The amount of salt transported out of the channel with salinity 35.2 is 2900 m^3 · 35.2 kg/m^3 = 102,080 kg. Thus, the salt transport is approximately balanced.

Conclusions

Tidal currents flow under ice in a shallow basin near the tip of the Van Mijen Fjord in Spitsbergen. The ice is almost aground but a small channel exists under ice. This channel was formed in summer time by a flow of freshwater from the mountains. During the flood cycle of tide seawater flows under ice approximately over a distance of one kilometer. Small amounts of seawater in the channel strongly freeze. Salinity of water increases due to salt rejection during freezing. During the ebb cycle, salinity of the outflowing water is greater than that of the inflowing water. Salt and mass balances are estimated. During high-water tide, salt water seeps through the cracks in the ice to the surface. This increase has been recorded by salinity sensors frozen in the ice near the surface.

Competing Interests

The authors do not have competing interests to declare.

Acknowledgments. The field works were supported by the Research Council of Norway through the SFI SAMCoT, IntPart project AOCEC. The analysis of the field data was supported by the Russian Science Foundation (grant No. 21-17-00278). The work was completed within State Assignment FMWE-2021-0002.

References

Bogorodskii, P. V., N. E. Demidov, K. V. Filchuk, A. V. Marchenko, E. G. Morozov, A. L. Nikulina, A. V. Pnyushkov, and I. V. Ryzhov, Growth of Landfast Ice and its Thermal Interaction with Bottom Sediments in the Braganzavågen Gulf (West Spitsbergen), *Russian Journal of Earth Sciences*, *20*, 6005, doi:10.2205/2020ES000718, 2020.

Cottier, F. R., F. Nilsen, R. Skogseth, V. Tverberg, J. Skarðhamar, and H. Svendsen, Arctic fjords: a review of the oceanographic environment and dominant physical processes, *Geological Society, London, Special Publications*, *344*(1), 35–50, doi:10.1144/sp344.4, 2010.

Høyland, K. V., Ice Thickness, Growth and Salinity in Van Mijenfjorden, Svalbard, Norway, *Polar Research*, *28*(3), 339–352, doi:10.3402/polar.v28i3.6141, 2009.

Høyland, K. V., and P. Liferov, On the Initial Phase of Consolidation, *Cold Regions Science and Technology*, *41*(1), 49–59, doi:10.1016/j.coldregions.2004.09.003, 2005.

Høyland, K. V., and S. Løset, Measurements of Temperature Distribution, Consolidation and Morphology of a First-Year Sea Ice Ridge, *Cold Regions Sci-*

ence and Technology, *29*(1), 59–74, doi:10.1016/S0165-232X(99)00004-X, 1999.

Launiainen, J., B. Cheng, J. Launiainen, and B. Cheng, Modelling of Ice Thermodynamics in Natural Water Bodies, *Cold Regions Science and Technology*, *27*(3), 153–178, doi:10.1016/S0165-232X(98)00009-3, 1998.

Leppäranta, M., A Review of Analytical Models of Sea-Ice Growth, *Atmosphere-Ocean*, *31*(1), 123–138, doi:10.1080/07055900.1993.9649465, 1993.

Liferov, P., K. V. Høyland, P. Liferov, and K. V. Høyland, In-Situ Ice Ridge Scour Tests: Experimental Set up and Basic Results, *Cold Regions Science and Technology*, *40*(1), 97–110, doi:10.1016/j.coldregions.2004.06.003, 2004.

Marchenko, A., E. Morozov, S. Muzylev, and S. Muzyleva, Measurements of Sea-Ice Flexural Stiffness by Pressure Characteristics of Flexural-Gravity Waves, *Annals of Glaciology*, *54*(64), 51–60, doi:10.3189/2013AoG64A075, 2013.

Marchenko, A. V., and E. G. Morozov, Surface Manifestations of the Waves in the Ocean Covered With Ice, *Russian Journal of Earth Sciences*, *16*(1), ES1001, doi:10.2205/2016ES000561, 2016.

Marchenko, A. V., E. G. Morozov, S. V. Muzylev, and A. S. Shestov, Interaction of Short Internal Waves with the Ice Cover in an Arctic Fjord, *Oceanology*, *50*(1), 18–27, doi:10.1134/S0001437010010029, 2010.

Marchenko, A. V., E. G. Morozov, A. V. Ivanov, T. G. Elizarova, and D. I. Frey, Ice Thickening Caused by Freezing of Tidal Jet, *Russian Journal of Earth Sciences*, *21*, ES2004, doi:10.2205/2021ES000761, 2021.

Morozov, E., A. Marchenko, K. Filchuk, Z. Kowalik, N. Marchenko, and I. Ryzhov, Sea Ice Evolution and Internal Wave Generation due to a Tidal Jet in a Frozen Sea, *Applied Ocean Research*, *87*, 179–191, doi:10.1016/j.apor.2019.03.024, 2019.

Morozov, E. G., S. V. Muzylev, A. S. Shestov, and A. V. Marchenko, Short-Period Internal Waves under an Ice Cover in Van Mijen Fjord, Svalbard, *Advances in Meteorology*, *2011*, 6, doi:10.1155/2011/573269, 2011.

Moslet, P. O., Medium Scale Ice–Structure Interaction, *Cold Regions Science and Technology*, *54*(2), 143–152, doi:10.1016/j.coldregions.2008.03.001, 2008.

Shestov, A., D. Wrangborg, and A. Marchenko, Hydrology of Braganzavågen under Ice-Covered Conditions, in *Proceedings of the International Conference on Port and Ocean Engineering under Arctic Conditions, POAC*, vol. 2015, 2015.

Skarðhamar, J., and H. Svendsen, Short-Term Hydrographic Variability in a Stratified Arctic Fjord, in *Fjord Systems and Archives*, Geological Society of London, doi:10.1144/SP344.5, 2010.

Stefan, J., Über die Theorie der Eisbildung, Insbesondere Über Eisbildung im Polarmeere, *Annalen der Physik*, *278*(2), 269–286, doi:10.1002/andp.18912780206, 1891.

Strub-Klein, L., and K. V. Høyland, Spatial and Temporal Distributions of Level Ice Properties: Experiments and Thermo-Mechanical Analysis, *Cold Regions Science and Technology*, *71*, 11–22, doi:10.1016/j.coldregions.2011.10.001, 2012.